Article type: Original Article

# Single View Echocardiographic Analysis for Left Ventricular Outflow Tract Obstruction Prediction in Hypertrophic Cardiomyopathy: A Deep Learning Approach

Jiesuck Park,[a,b†] Jiyeon Kim,[c†] Jaeik Jeon,[c*] Yeonyee E. Yoon,[a,b,c*] Yeonggul Jang,[c] Hyunseok Jeong,[d,e] Seung-Ah Lee,[c,d] Hong-Mi Choi,[a,b] In-Chang Hwang,[a,b] Goo-Yeong Cho,[a,b] Hyuk-Jae Chang[c,d,f]

[a]Cardiovascular Center and Division of Cardiology, Department of Internal Medicine, Seoul National University Bundang Hospital, Seongnam, Gyeonggi, Republic of Korea

[b]Department of Internal Medicine, Seoul National University College of Medicine, Seoul, Republic of Korea

[c]Ontact Health Inc., Seoul, Republic of Korea

[d]CONNECT-AI Research Center, Yonsei University College of Medicine, Seoul, Republic of Korea

[e]Department of Internal Medicine, Graduate School of Medical Science, Brain Korea 21 Project, Yonsei University College of Medicine, Seoul, Republic of Korea

[f]Division of Cardiology, Severance Cardiovascular Hospital, Yonsei University College of Medicine, Yonsei University Health System, Seoul, Republic of Korea

[†]The first two authors contributed equally to this work.

**Running title:** DL Prediction of LVOT Obstruction in HCM

***Corresponding authors:**

Yeonyee E. Yoon, MD, PhD

Professor, Division of Cardiology, Cardiovascular Center

Seoul National University Bundang Hospital

82, 173 Beon-gil, Gumi-ro, Bundang-gu, Seongnam-si, Gyeonggi-do, Republic of Korea

Phone: 82-31-787-7072

Email: yeonyeeyoon@snubh.org

And

Jaeik Jeon, MSc

Ontact Health Inc., Seoul, Republic of Korea

50-5, Ewhayeodae-gil, Seodaemun-gu, Seoul, Republic of Korea

Phone: 82-2-362-9610

E-mail: jaeikjeon9919@gmail.com

**Fundings:** This work was supported by a grant from the Institute of Information & communications Technology Planning & Evaluation (IITP) funded by the Korea government (Ministry of Science and ICT) (No.2022000972, Development of a Flexible Mobile Healthcare Software Platform Using 5G MEC); and the Medical AI Clinic Program through the NIPA funded by the MSIT. (Grant No.: H0904-24-1002).

**ABSTRACT**

**Background**: Accurate left ventricular outflow tract obstruction (LVOTO) assessment is crucial for hypertrophic cardiomyopathy (HCM) management and prognosis. Traditional methods often require multiple echocardiographic views, Doppler imaging, and provocation maneuvers, which may not always be feasible or readily available.

**Objective**: To develop and validate a deep learning (DL) model capable of predicting severe LVOTO in HCM patients using only the parasternal long-axis (PLAX) view from transthoracic echocardiography (TTE).

**Methods**: A DL model was trained on PLAX videos (developmental dataset, n=1,007) to capture both morphological and dynamic motion features for predicting severe LVOTO, generating a DL index for LVOTO (DLi-LVOTO, range 0-100). Performance was evaluated in an internal test dataset (ITDS, n=87) and externally validated in the distinct hospital dataset (DHDS, n=1,334) and the LVOTO reduction treatment dataset (n=156).

**Results**: The DL model achieved high accuracy in detecting severe LVOTO, with an area under the receiver operating characteristics curve (AUROC) of 0.96 (95% confidence interval: 0.92-0.99) in ITDS and 0.91 (0.89-0.93) in DHDS. At a DLi-LVOTO threshold of 50, the model demonstrated high specificity 97.3% and negative predictive value (NPV) of 93.6% in ITDS, and a 92.2% specificity and 95.5% NPV in DHDS. In the LVOTO reduction treatment dataset, DLi-LVOT showed a marked decrease following both surgical myectomy and Mavacamten treatment, correlating with reductions in peak pressure gradient ($p<0.001$ for all).

**Conclusions**: Our DL-based approach predicts severe LVOTO using only the PLAX view from TTE, serving as a complementary tool when conventional Doppler evaluation is limited and for monitoring treatment response.

**Keywords:** Hypertrophic cardiomyopathy; deep learning; echocardiography; left ventricular outflow tract obstruction; prediction

## 1. INTRODUCTION

Hypertrophic cardiomyopathy (HCM) is one of the most common genetic cardiomyopathies, with an estimated prevalence of 1 in 200 to 1 in 500.[1] The phenotype of HCM is highly heterogeneous, ranging from asymptomatic presentation to severe outcomes such as sudden cardiac death (SCD). Among the various factors influencing symptoms and prognosis, left ventricular outflow tract (LVOT) obstruction (LVOTO) plays a pivotal role.[1,2] When LVOTO becomes severe, it not only contributes to symptoms such as exertional dyspnea, chest pain, and syncope but also serves as the key determinant in guiding clinical management, including pharmacological treatment, septal reduction intervention, or surgery.[2] Therefore, accurate identification of LVOTO is critical in the clinical evaluation of HCM patients.

Transthoracic echocardiography (TTE) is the primary imaging modality for diagnosing and evaluating HCM.[2] LVOTO is typically assessed through TTE using Doppler imaging and multiple echocardiographic views, often incorporating provocation maneuvers.[2] However, these assessments require significant expertise, are time-consuming, and are subject to technical variability and interobserver differences, which may limit their feasibility in certain clinical settings. Among TTE views, the parasternal long axis (PLAX) view is one of the most fundamental, offering critical insights into cardiac anatomy and dynamic function. Therefore, leveraging this single, widely available view for automated prediction of LVOTO could improve accessibility and maintain clinical accuracy, even in settings where expert evaluation is limited or advanced Doppler-equipped systems are unavailable.

Recent advancements in deep learning (DL) have demonstrated significant potential in automating and enhancing medical image interpretation, and TTE is no exception. DL algorithms can identify complex patterns in imaging data that may elude human observers, thereby improving diagnostic accuracy and efficiency. For instance, efforts have been made to

accurately assess conditions such as aortic stenosis and diastolic dysfunction using limited 2-dimensional (2D) TTE images, even without Doppler input.[3-6] Despite these advances, the application of DL for predicting LVOTO using single-view TTE in HCM patients remains underexplored.

In the present study, we hypothesized that a DL model trained on 2D PLAX TTE videos can reliably predict the presence of severe LVOTO in HCM patients without requiring Doppler input. We propose a novel multi-resolution motion feature extraction framework, generating M-mode representation to better capture the subtle dynamics indicative of severe LVOTO, thereby improving model performance and interpretability. This paper outlines the development and validation of our DL-based model and demonstrates its predictive capability for severe LVOTO in HCM patients. We aim to evaluate whether this approach could serve as a reliable and efficient alternative to conventional Doppler-based assessment, which typically requires multiple TTE views with various provocation maneuvers.

## 2. METHODS

### 2.1. Study Population and Data Sources

The DL-based model presented in this study was developed and validated using the Open AI Dataset Project (AI-Hub) dataset, an initiative supported by the South Korean government's Ministry of Science and ICT.[5,7-11] This dataset included 30,000 echocardiographic examinations retrospectively collected from five tertiary hospitals between 2012 and 2021, encompassing a wide range of cardiovascular diseases, including HCM. From this dataset, we reviewed cases categorized as HCM. The inclusion criteria required that echocardiographic reports were as follows: (1) availability of echocardiographic reports, (2) a clinical diagnosis of HCM established by identifying a maximal end-diastolic wall thickness >15mm in any segment of the left ventricle (LV), with other potential causes of hypertrophy excluded, and (3) TTE in which the presence or absence of LVOTO had been assessed.

To develop the DL-based LVOTO prediction algorithm, we created the Developmental Dataset (DDS), consisting of 722 patients with 1,007 TTE examinations, which were divided into training, validation, and test datasets in an 8:1:1 ratio, comprising 578, 71, and 73 patients (809, 111, and 87 TTE examinations, respectively). (**Figure 1**) Notably, data from Severance Hospital was excluded from the DDS and instead designated as the Distinct Hospital Dataset (DHDS) for independent external tests. The DHDS included 573 patients with 1,334 TTE examinations used solely for external validation. Additionally, we collected TTE data from obstructive HCM patients who underwent LVOT gradient reduction treatment at Seoul National University Bundang Hospital and Severance Hospital. This dataset comprises 18 patients with 115 TTE examinations from those who underwent surgical myectomy and 13 patients with 45 TTE examinations from those treated with Mavacamten. To prevent potential bias in DL model training, patients included in these datasets were excluded from the DDS,

regardless of the timing of their TTE examinations.

The study protocol was approved by the Institutional Review Board of Seoul National University Bundang Hospital (IRB No. B-2305-827-002, and B-2503-959-104), with a waiver of informed consent granted due to the retrospective study design. All clinical data were fully anonymized prior to analysis. The study was conducted in accordance with the principles outlined in the Declaration of Helsinki (2013).

### 2.2. TTE Acquisition and Interpretation

All TTE studies were conducted by trained echocardiographers or cardiologists and interpreted by board-certified cardiologists specializing in echocardiography as part of routine clinical care. All TTE examinations included in this study were standard TTEs; exercise or pharmacological stress tests were not included. However, simple provocation maneuvers such as the Valsalva, which can be easily performed during standard TTE, were included to evaluate LVOTO. For the assessment of LVOTO, continuous-wave Doppler was used in the apical 3-chamber or 5-chamber view to measure the LVOT peak velocity ($V_{max}$, m/sec). The Bernoulli equation ($PG = 4 \times Vmax^2$) was then applied to calculate the LVOT peak PG. LVOTO was classified based on the LVOT peak pressure gradient (PG): a peak PG ≥ 30mmHg was defined as significant LVOTO, and a peak PG ≥ 50mmHg was defined as severe LVOTO.[2,12]

### 2.3. Model Development

We developed a novel DL model to predict severe LVOTO using single-view, 2D PLAX TTE videos, eliminating the need for Doppler assessments. The model was explicitly designed to capture both morphological and M(otion)-mode features critical for LVOTO assessment.

(**Figure 2**)

Our network architecture was based on a modified version of R(2+1)D-18 as the primary backbone.[13] This architecture is based on a ResNet-18[14] but uses 3-dimensional (3D) convolutions factorized into 2D spatial + 1-dimensional (1D) temporal components but is modified to retain full temporal resolution for video data. To capture motion dynamics critical for predicting severe LVOTO, we introduced an automated M-mode generation process that leverages a spatial transformer network (STN).[15] Instead of requiring a clinician to position the M-mode line manually, our model learns to predict the optimal M-mode line and extract the motion information along that line in a fully differentiable manner. The generated M-mode representations were independently processed using a pre-trained EfficientNet.[8,16] Bilinear pooling is then applied to fuse the B-mode (video) and M-mode features, effectively encoding how each structural feature correlates with each motion feature. We incorporate an auxiliary loss that nudges it toward a known reference line to ensure that the M-mode trajectory is anatomically meaningful. Specifically, an auxiliary mean squared error (MSE) was applied to constrain the M-mode trajectory to pass through the mitral valve (MV) tip, ensuring alignment with anatomical landmarks that influence LVOTO. This integration enabled the model to focus on clinically meaningful motion patterns rather than solely on data-driven feature selection.

The model was trained using a supervised learning approach with a primary classification task to distinguish severe and non-severe LVOTO, optimized using a binary cross-entropy (CE) loss. Since severe LVOT obstruction is defined based on peak PG, which can be augmented by provocation, but PLAX videos used in this study were recorded at rest, we introduced an auxiliary regression task to predict the LVOT PG measured at rest. This guided the network to learn subtle hemodynamic features from resting images that correlate with obstruction severity, allowing it to infer additional predictive cues beyond rest-only inputs

for a diagnosis that often requires provocation. Overall, the training objective was formulated as a weighted combination of three loss components: binary CE loss for classification, mean absolute error (MAE) loss for PG regression, and anatomical MSE loss to ensure physiologically meaningful feature extraction.

For patient-level DLi-LVOTO (range 0-100), multiple PLAX videos from a single patient were individually analyzed, and their DLi-LVOTO scores were averaged. The model represents the latest advancement in our artificial intelligence (AI)-driven HCM evaluation module (USfeat_HCM.ai, Ontact Health, Korea), which integrates validated features such as view classification and automatic measurement capabilities.[8,10,11,17]

### 2.4. Model Validation and Statistical Analysis

The performance of our DL-based LVOTO prediction model was validated using an internal test dataset (ITDS) and an independent external dataset (DHDS). Additionally, we assessed the model's performance in serial TTE examinations of patients who underwent LVOT gradient reduction therapy, including surgical myectomy and Mavacamten treatment.

The DL-based prediction algorithm's performance for severe LVOTO in the ITDS and DHDS was evaluated using receiver operating characteristics (ROC) curve analysis, with the area under the curve (AUC) and 95% confidence interval (CI) as key performance measures. We also visualized the distribution of the DLi-LVOTO across categories of no or insignificant LVOTO, significant LVOTO, and severe LVOTO using violin plots. Additionally, we stratified DLi-LVOTO into 10-unit intervals and evaluated its diagnostic performance at each cutoff, assessing key performance metrics, including accuracy, F1-score, sensitivity, specificity, positive predictive value (PPV), and negative predictive value (NPV). Saliency maps were

generated using the Gradient-weighted Class Activation Mapping (Grad-CAM)[18], with representative maps presented for each severity level to highlight the areas with the greatest influence on the model's prediction. In patients who were treated with surgical myectomy or Mavacamten, we compared baseline and FU TTE studies performed before and after treatment by visualizing changes in LVOT peak PG and DLi-LVOTO.

## 3. RESULTS

### 3.1. Baseline Clinical and Echocardiographic Characteristics

Baseline clinical and echocardiographic characteristics across datasets are shown in **Table 1**. Overall, the DDS exhibited a relatively balanced distribution of apical, septal, and diffuse or mixed types of HCM. However, in the DHDS, the septal type was the most prevalent. Regarding significant LVOTO prevalence, DDS showed a 27-29% prevalence, whereas DHDS had a lower prevalence of 15.4%. Additionally, when comparing the Mavacamten treatment dataset and the surgical myectomy dataset, patients who received Mavacamten were generally older and had a higher diffuse or mixed-type prevalence. In contrast, those who underwent surgical myectomy were relatively younger, with a predominance of the septal type.

### 3.2. Performance of DL-based prediction of LVOT obstruction

Our DL-based LVOTO prediction model was able to reliably detect the presence of severe LVOTO using single-view, 2D PLAX videos, achieving an AUROC of 0.96 (95% CI: 0.92-0.99) in ITDS and 0.91 (95% CI: 0.89-0.93) in DHDS. (**Figure 3**) The DLi-LVOTO distribution showed a gradual increase with LVOTO severity in both ITDS and DHDS, reflecting a consistent relationship between the predicted scores and clinical classification (**Figure 3**).

**Table 2** presents the diagnostic performance of DLi-LVOTO across different cutoff values for identifying severe LVOTO in both the ITDS and DHDS. In the ITDS, the highest accuracy (92.0%) was observed at a DLi-LVOTO cutoff of 50, demonstrating excellent specificity (97.3%) and NPV (93.6%). These results suggest that when DLi-LVOTO is low, severe LVOTO can be safely ruled out, highlighting the model's potential as a gatekeeper. This

trend was consistently reproduced in the DHDS, where applying the same cutoff of 50 resulted in an accuracy of 89.3%, with a specificity of 92.2 and an NPV of 95.5%.

For each severity level, we present representative samples with Grad-CAM saliency maps overlaid on PLAX views, specifically highlighting the LVOT region (**Figure 4**). These results demonstrate that our model accurately identifies the relevant regions for evaluating LVOTO across all severity levels without supervision.

### 3.3. DLi-LVOTO Changes After LVOT Gradient Reduction Treatment

In patients who underwent LVOT gradient reduction treatment, we visualized the changes in LVOT peak PG and DLi-LVOTO between baseline and FU TTE exams (**Figure 5**). In patients who underwent surgical myectomy, LVOT peak PG showed a marked reduction post-surgery, accompanied by a corresponding decrease in DLi-LVOTO. Similarly, in patients treated with Mavacamten, both LVOT peak PG and DLi-LVOTO progressively decreased over the course of treatment compared to baseline. Representative cases are presented in **Figure 6**. In the patient who underwent surgical myectomy, a significant reduction in peak PG was accompanied by a corresponding decrease in DLi-LVOTO. In a while, for the patient treated with Mavacamten, when the initial treatment response was insufficient, both peak PG and DLi-LVOTO remained elevated. The results demonstrated that changes in DLi-LVOTO closely paralleled changes in LVOT peak PG following treatment.

## 4. DISCUSSION

We have developed and validated a DL-based model for predicting severe LVOTO in HCM using only a single TTE view. Despite relying solely on the PLAX view, the model demonstrated high accuracy in predicting severe LVOTO, with robust performance validated not only in the ITDS but also in independent external datasets. These findings suggest that this approach could be a reliable and efficient alternative to conventional methods. Furthermore, we observed that changes in LVOT peak PG following treatment correlated with corresponding changes in DLi-LVOTO within the same patient, highlighting the model's potential utility in tracking treatment response.

The application of artificial intelligence (AI) in echocardiography has significantly progressed over the past decade. Early AI research primarily focused on automating manual measurements, including view classification, target structure segmentation, and automatic quantification. However, one of the core aspects of echocardiographic examination – the expert-driven visual analysis – remained largely unchallenged by AI. Recently, with advancements in DL, models that mimic expert eyeball analysis have begun to emerge. Notable examples include models that predict diastolic dysfunction from an apical 4-chamber view and those that assess aortic stenosis using PLAX and/or parasternal short-axis views.[4-6,19] These models do not aim for a standalone definitive diagnosis but rather serve as decision-support tools, similar to eyeball evaluation, by flagging potential disease presence and guiding further workup. Such DL-driven approaches are particularly valuable in settings where expert interpretation is unavailable or where equipment is limited, such as when only handheld ultrasound devices without Doppler capabilities are available. In these cases, DL-based assessments can help identify at-risk patients and facilitate appropriate referrals to specialized centers.

In line with this evolving AI paradigm, we sought to develop a DL model capable of predicting LVOTO, a key determinant of HCM management and prognosis, using only the PLAX view. However, unlike aortic stenosis, which is typically a fixed obstruction, LVOTO is inherently dynamic, fluctuating significantly throughout the day and influenced by physiological and hemodynamic conditions. Therefore, accurate LVOTO assessment with TTE typically requires provocation maneuvers, such as the Valsalva maneuver, to induce obstruction and unmask its severity. Given this variability, predicting LVOTO using only resting B-mode TTE videos may be challenging even without color or spectral Doppler input. However, certain structural and hemodynamic factors that predispose patients to LVOTO development can still be evaluated on resting TTE. These include a narrowed LVOT, sigmoid septum morphology, systolic anterior motion of the MV, and small LV cavity size, all of which contribute to flow acceleration and obstruction under specific conditions. Building on this premise, we hypothesized that the PLAX view – a foundational TTE view and the starting point of TTE assessment – could serve as a suitable input for AI-based LVOTO prediction. The PLAX view clearly visualizes the LVOT and key anatomical determinants of obstruction, making it an optimal input for LVOTO assessment. As a result, we successfully developed a DL-based model trained on single-view video data that can reliably identify severe LVOTO, even without the need for Doppler input or multi-view analysis.

Several previous studies on echocardiographic disease prediction have adopted different strategies, each with inherent limitations. For example, Huang et al. [ref] extracted single frames from echocardiogram videos, converted them to grayscale, and resized them to 64×64 pixels before training a WideResNet-28 for view classification and aortic stenosis diagnosis. While this 2D method is computationally efficient, its static nature makes capturing the dynamic motion patterns critical for conditions like LVOTO challenging. In contrast, Holste et al.[4] employed 3D convolutional neural networks (CNNs) with extensive self-supervised

pretraining and deep ensemble methods, assuming that temporal patterns would emerge implicitly from the video data. Although such approaches benefitted from modeling spatiotemporal information, they did not explicitly focus on the motion of key anatomical structures and were computationally expensive. Similarly, our group previously utilized an R(2+1)D architecture with a continuum-aware multi-task loss to accurately classify and comprehensively assess the aortic valve stenosis continuum.[5] However, this method still relied on the network to implicitly learn temporal dynamics rather than explicitly track motion. In contrast, our current LVOTO prediction model was explicitly designed to capture both morphological and dynamic motion features crucial for LVOTO assessment. By incorporating multi-level M-mode generation and embeddings, our method enhances the detection of subtle transient motion, such as the SAM of the MV, and their resulting hemodynamic consequences.

While B-mode-derived M-mode representations have been explored in AI-driven echocardiographic analysis, the prior approach has limitations. For instance, a previous study attempted to improve cardiac function prediction by incorporating M-mode imaging for ejection fraction estimation.[20] However, their method relied on fixed sampling lines selected via heuristic rules, producing static M-mode representations that could not adapt to individual patient anatomy or dynamic motion patterns. Additionally, because M-mode extraction was performed as a separate preprocessing step, the model could not refine feature selection end-to-end manner, potentially limiting diagnostic performance. In contrast, using a spatial transformer module, our proposed approach directly integrates M-mode generation into the DL framework. This design allows the network to dynamically determine each video frame's most informative M-mode trajectory, ensuring that key motion features are consistently captured. By jointly optimizing the trajectory selection, feature extraction, and classification, our model overcomes the constraints of the static M-mode placement and enables more robust LVOTO detection. Furthermore, beyond traditional M-mode techniques, our model further enhances

feature extractions through multi-resolution processing and bilinear fusion of B-mode and M-mode representations, providing a comprehensive understanding of both structural morphology and motion dynamics within an end-to-end framework. This integration improves classification accuracy and enhances clinical interpretability, as the network autonomously identifies and prioritizes diagnostically relevant features directly from the data. Importantly, our automated M-mode generation yields visualizations that align with traditional clinical practice, where M-mode imaging is highly valued for capturing motion over time by producing M-mode images that display critical dynamic features in a format familiar to clinicians. Moreover, Grad-CAM overlays on these generated M-mode images further enhance interpretability by highlighting the precise regions and moments of abnormal motion that drive the network's predictions.

This study has several limitations. Although we developed and rigorously validated our DL-based model using multi-center data, including internal and external validation, all datasets were retrospectively collected from tertiary centers in South Korea. As a result, caution is required when interpreting the findings and applying them to clinical practice. Further validation across diverse populations and healthcare settings is essential to enhance generalizability. Additionally, while the DL model was evaluated using TTE data from multiple institutions, its performance in resource-limited environments or when used by novice operators remains uncertain. Whether DLi-LVOTO will perform reliably on TTE images acquired in such settings is yet to be determined. However, given that the PLAX view is one of the most fundamental TTE views and is more likely to be adequately obtained than a complete multi-view TTE examination, this suggests that DLi-LVOTO could provide a reliable assessment of LVOTO in HCM patients even in less advanced settings. Secondly, LVOTO is not exclusive to HCM patients and can occur in various clinical settings, such as hyperdynamic states and certain cardiac structural variations. Additional studies are required to determine whether DLi-LVOTO can accurately detect LVOTO in non-HCM patients. Thirdly, this study

also examined the changes in DLi-LVOTO in response to Mavacamten or surgical myectomy treatment alongside LVOT PG, but the analysis was conducted on a relatively small patient cohort. Larger scale studies are needed to confirm the reproducibility of these observations. Lastly, future research should explore whether DLi-LVOTO can predict clinical outcomes in HCM patients. Addressing these aspects will be crucial for further validating the clinical utility of this DL-based approach.

In conclusion, our DL-based approach enables the prediction of severe LVOTO using only the PLAX view from TTE, providing a complementary tool in situations where acquiring multiple views or Doppler-based LVOT pressure gradients is challenging. Additionally, DLi-LVOTO may aid in monitoring treatment response, offering insights into hemodynamic changes following surgical myectomy or Mavacamten therapy. This method has the potential to enhance LVOTO evaluation in select clinical scenarios, supporting rather than replacing traditional assessment methods.

## Contributors

All authors contributed equally to this study. All authors have read and approved the final version of the manuscript. J.P, J.K, J.J, and Y.E.Y verified the underlying data of the current study.

## Data Sharing Statement

The AI-Hub data may be accessible upon proper request and after approval of a proposal. Data from TDDS cannot be made publicly available due to ethical restrictions set by the IRB of the study institution; i.e., public availability would compromise patient confidentiality and participant privacy. Please contact the corresponding author (yeonyeeyoon@gmail.com) to request the minimal anonymized dataset. Researchers with additional inquiries about the deep learning model developed in this study are also encouraged to reach out to the corresponding author.

## Declaration of Interests

Y.E.Y, J.J., Y.J., Y.H., and S.A.L. are currently affiliated with Ontact Health, Inc. J.J., J.K., and S.A.L are co-inventors on a patent related to this work filed by Ontact Health (Method For Providing Information On Severity Of Aortic Stenosis And Device Using The Same). H.J.C. holds stock in Ontact Health, Inc. The other authors have no conflicts of interest to declare.

## Acknowledgements

This work was supported by a grant from the Institute of Information & communications Technology Planning & Evaluation (IITP) funded by the Korea government (Ministry of Science and ICT) (No.2022000972, Development of a Flexible Mobile Healthcare Software Platform Using 5G MEC); and the Medical AI Clinic Program through the NIPA funded by the MSIT. (Grant No.: H0904-24-1002).

**REFERENCES**


1. Maron BJ, Desai MY, Nishimura RA, Spirito P, Rakowski H, Towbin JA, et al. Diagnosis and Evaluation of Hypertrophic Cardiomyopathy: JACC State-of-the-Art Review. *J Am Coll Cardiol*. 2022;79:372–389.

2. Abbasi M, Ong KC, Newman DB, Dearani JA, Schaff HV, Geske JB. Obstruction in Hypertrophic Cardiomyopathy: Many Faces. *J Am Soc Echocardiogr*. 2024;37:613–625.

3. Wessler BS, Huang Z, Long GM Jr, Pacifici S, Prashar N, Karmiy S, et al. Automated Detection of Aortic Stenosis Using Machine Learning. *J Am Soc Echocardiogr*. 2023;36:411–420.

4. Holste G, Oikonomou EK, Mortazavi BJ, Coppi A, Faridi KF, Miller EJ, et al. Severe aortic stenosis detection by deep learning applied to echocardiography. *Eur Heart J*. 2023;44:4592–4604.

5. Park J, Kim J, Jeon J, Yoon YE, Jang Y, Jeong H, et al. Artificial intelligence-enhanced comprehensive assessment of the aortic valve stenosis continuum in echocardiography. *EBioMedicine*. 2025;112:105560.

6. Chen X, Yang F, Zhang P, Lin X, Wang W, Pu H, et al. Artificial Intelligence-Assisted Left Ventricular Diastolic Function Assessment and Grading: Multiview Versus Single View. J Am Soc Echocardiogr. 2023;36:1064–1078.

7. National Information Society Agency. Open AI Dataset Project (AI-Hub). https://aihub.or.kr/.

8. Jeon J, Ha S, Yoon YE, Kim J, Jeong H, Jeong D, et al. Echocardiographic view classification with integrated out-of-distribution detection for enhanced automatic echocardiographic analysis. *arXiv [eess.SP; 2023]. Available from: https://arxiv.org/abs/2308.16483.*

9. Jeon J, Kim J, Jang Y, Yoon YE, Jeon D, Hong Y, et al. A Unified Approach for Comprehensive Analysis of Various Spectral and Tissue Doppler Echocardiography. *arXiv [eess.IV; 2023]. Available from: https://arxiv.org/abs/2311.08439.*

10. Park J, Jeon J, Yoon YE, Jang Y, Kim J, Jeong D, et al. Artificial intelligence-enhanced automation of left ventricular diastolic assessment: a pilot study for feasibility, diagnostic validation, and outcome prediction. *Cardiovasc Diagn Ther*. 2024;14:352–366.

11. Jang Y, Choi H, Yoon YE, Jeon J, Kim H, Kim J, et al. An Artificial Intelligence-Based Automated Echocardiographic Analysis: Enhancing Efficiency and Prognostic Evaluation in Patients With Revascularized STEMI. *Korean Circ J*. 2024;54:e103.

12. Ommen SR, Ho CY, Asif IM, Balaji S, Burke MA, Day SM, et al. 2024 AHA/ACC/AMSSM/HRS/PACES/SCMR Guideline for the Management of Hypertrophic Cardiomyopathy: A Report of the American Heart Association/American College of Cardiology Joint Committee on Clinical Practice Guidelines. *Circulation*. 2024;149:e1239–e1311.

13. Tran D, Wang H, Torresani L, Ray J, LeCun Y and Paluri M. A Closer Look at Spatiotemporal Convolutions for Action Recognition. *2018 IEEE/CVF Conference on Computer Vision and Pattern Recognition*, Salt Lake City, UT, USA. 2018:6450–6459.

14. He K, Zhang X, Ren S and Sun J. Deep Residual Learning for Image Recognition. *2016 IEEE Conference on Computer Vision and Pattern Recognition*, Las Vegas, NV, USA. 2016:770–778.

15. Jaderberg M, Simonyan K, Zisserman A and Kavukcuoglu K. Spatial Transformer Networks. *arXiv [cs.CV; 2015]. Available from: https://arxiv.org/abs/1506.02025*.

16. Tan M and Le Q. EfficientNet: Rethinking Model Scaling for Convolutional Neural Network. *arXiv [cs.LG; 2019]. Available from: https://arxiv.org/abs/1905.11946*.

17. Park J, Yoon YE, Jang Y, Jung T, Hong Y, Lee SA et al. Novel Deep Learning Framework for Simultaneous Assessment of Left Ventricular Mass and Longitudinal Strain: Clinical Feasibility and Validation in Patients with Hypertrophic Cardiomyopathy. *medRxiv [2025]. Available from: https://www.medrxiv.org/content/10.1101/2025.01.17.25320694v1*.

18. Selvaraju RR, Cogswell M, Das A, Vedantam R, Parikh D, Batra D. Grad-CAM: visual explanations from deep networks via gradient-based localization. *International journal of computer vision*. 2020;128:336–359.

19. Huang Z, Long G, Wessler B and Hughes MC. A New Semi-supervised Learning Benchmark for Classifying View and Diagnosing Aortic Stenosis from Echocardiograms. *Proceedings of the 6th Machine Learning for Healthcare Conference*. 2021;149:614–647.

20. Ozkan E, Sutter TM, Hu Y, Balzer S and Vogt JE. M(otion)-mode Based Prediction of Ejection Fraction using Echocardiograms. *arXiv [eess.IV; 2023]. https://arxiv.org/abs/2309.03759.*

## Table 1. Baseline Characteristics

| | Developmental Dataset | | | External Test Dataset | | |
|---|---|---|---|---|---|---|
| | Training Dataset | Validation Dataset | Internal Test Dataset (ITDS) | Distinct Hospital Dataset (DHDS) | Surgical Myectomy Dataset | Mavacamten Treatment Dataset |
| *Demographics* | | | | | | |
| Number of patients | 578 | 71 | 73 | 573 | 17 | 13 |
| | 65 (55–74) | 60 (51–72) | 65 (56–75) | 60 (50–70) | 60 (46–65) | 69 (51–77) |
| Male | 385 (66.6) | 385 (66.6) | 55 (77.5) | | | |
| HCM type | | | | 384 (67.0) | 9 (52.9) | 6 (46.2) |
| Apical | 226 (39.1) | 226 (39.1) | 24 (33.8) | 114 (19.9) | 0 (0.0) | 0 (0.0) |
| Spetal | 178 (30.8) | 178 (30.8) | 24 (33.8) | 409 (71.4) | 10 (58.8) | 3 (23.1) |
| Diffuse or mixed | 161 (27.9) | 161 (27.9) | 23 (32.4) | 40 (7.0) | 7 (41.2) | 9 (69.2) |
| Others | 13 (2.2) | 13 (2.2) | 0 (0.0) | 10 (1.7) | 0 (0.0) | 1 (7.7) |
| *Echocardiographic data* | | | | | | |
| Number of TTEs | 809 | 111 | 87 | 1,334 | 112 | 44 |
| LVEDD, mm | 45 (41–48) | 45 (42–48) | 46 (42–50) | 47 (44–51) | 44 (40–49) | 42 (37–46) |
| IVS, mm | 15 (12–18) | 16 (14–18) | 14 (12–18) | 18 (16–20) | 17 (15–20) | 18 (14-22) |
| LVEF, % | 65 (61–69) | 65 (61–69) | 65 (62–69) | 68 (62–73) | 65 (58–69) | 67 (62–69) |
| LAVI, ml/m$^2$ | 45 (36–58) | 48 (39–59) | 47 (38 –60) | 44 (35–56) | 59 (42–77) | 54 (46–79) |
| E/e | 13 (10–18) | 13 (10–17) | 13 (9–18) | 15 (11–19) | 19 (15–24) | 19 (13–29) |
| LVOTO | 235 (29.0) | 31 (27.9) | 24 (27.6) | 205 (15.4) | 55 (49.1) | 26 (59.1) |
| Significant (30≤ to <50mmHg) | 73 (9.0) | 13 (11.7) | 12 (13.8) | 48 (3.6) | 13 (11.6) | 9 (20.5) |
| Severe (≥50mmHg) | 162 (20.0) | 18 (16.2) | 12 (13.8) | 157 (11.8) | 42 (37.5) | 17 (38.6) |
| SAM | 97 (12.0) | 6 (5.4) | 7 (8.0) | 163 (12.2) | 43 (38.4) | 21 (47.7) |

Values are given as numbers (percentage) or median (interquartile range).
Abbreviations: E/e, ratio of early diastolic mitral inflow velocity to early diastolic mitral annular velocity; HCM, hypertrophic cardiomyopathy; IVS, interventricular septum; LAVI, left atrial volume index; LVEDD, left ventricular end-diastolic dimension; LVEF, left ventricular ejection fraction; LVOTO, left ventricular outflow tract obstruction; SAM, systolic anterior motion; TTE, transthoracic echocardiography.

**Table 2. Diagnostic Performance of DLi-LVOTO Cutoffs for Identifying Severe LVOTO**

| | Internal Test Dataset (ITDS) | | | | | | Distinct Hospital Dataset (DHDS) | | | | | |
|---|---|---|---|---|---|---|---|---|---|---|---|---|
| DLi-LVOTO Cutoff | Accuracy (%) | F1-score | Sensitivity (%) | Specificity (%) | PPV (%) | NPV (%) | Accuracy (%) | F1-score | Sensitivity (%) | Specificity (%) | PPV (%) | NPV (%) |
| 10 | 50.6 | 35.8 | **100.0** | 42.7 | 21.8 | **100.0** | 61.6 | 37.3 | **96.8** | 56.9 | 23.1 | **99.3** |
| 20 | 69.0 | 47.1 | **100.0** | 64.0 | 30.8 | **100.0** | 76.3 | 47.5 | 91.1 | 74.3 | 32.1 | 98.4 |
| 30 | 85.1 | 64.9 | **100.0** | 82.7 | 48.0 | **100.0** | 82.2 | 52.3 | 82.8 | 82.2 | 38.2 | 97.3 |
| 40 | 88.5 | **66.7** | 83.3 | 89.3 | 55.6 | 97.1 | 86.2 | 56.6 | 76.4 | 87.5 | 44.9 | 96.5 |
| 50 | **92.0** | **66.7** | 58.3 | 97.3 | 77.8 | 93.6 | 89.3 | **59.7** | 67.5 | 92.2 | 53.5 | 95.5 |
| 60 | 89.7 | 52.7 | 41.7 | 97.3 | 71.4 | 91.2 | 90.3 | 57.1 | 54.8 | 95.1 | 59.7 | 94.0 |
| 70 | 89.7 | 52.7 | 41.7 | 97.3 | 71.4 | 91.2 | **90.5** | 52.0 | 43.9 | 96.7 | 63.9 | 92.8 |
| 80 | 88.5 | 28.6 | 16.7 | **100.0** | **100.0** | 88.2 | 90.0 | 40.9 | 29.3 | **98.1** | **67.6** | 91.2 |

Abbreviations: NPV, negative predictive value; PPV, positive predictive value.

**Figure Legend**

**Figure 1. Overview of Dataset Composition for DL-Based LVOTO Prediction Model Development and Validation**

This figure illustrates the composition of datasets used for the development and validation of the DL-based LVOTO prediction model. The Developmental Dataset (DDS) was derived from multiple tertiary hospitals, excluding data from Severance Hospital, which was designated as the Distinct Hospital Dataset (DHDS) for independent external validation.

Additionally, we collected baseline and follow-up TTE data from obstructive HCM patients who underwent surgical myectomy or Mavacamten treatment, forming the Surgical Myectomy Dataset and Mavacamten Treatment Dataset, respectively. Each dataset is independent, and no patients were shared across datasets to prevent data leakage and ensure unbiased model training and evaluation.

DL, deep learning; LVOTO, left ventricular outflow tract obstruction; SNUBH, Seoul National University Bundang Hospital.

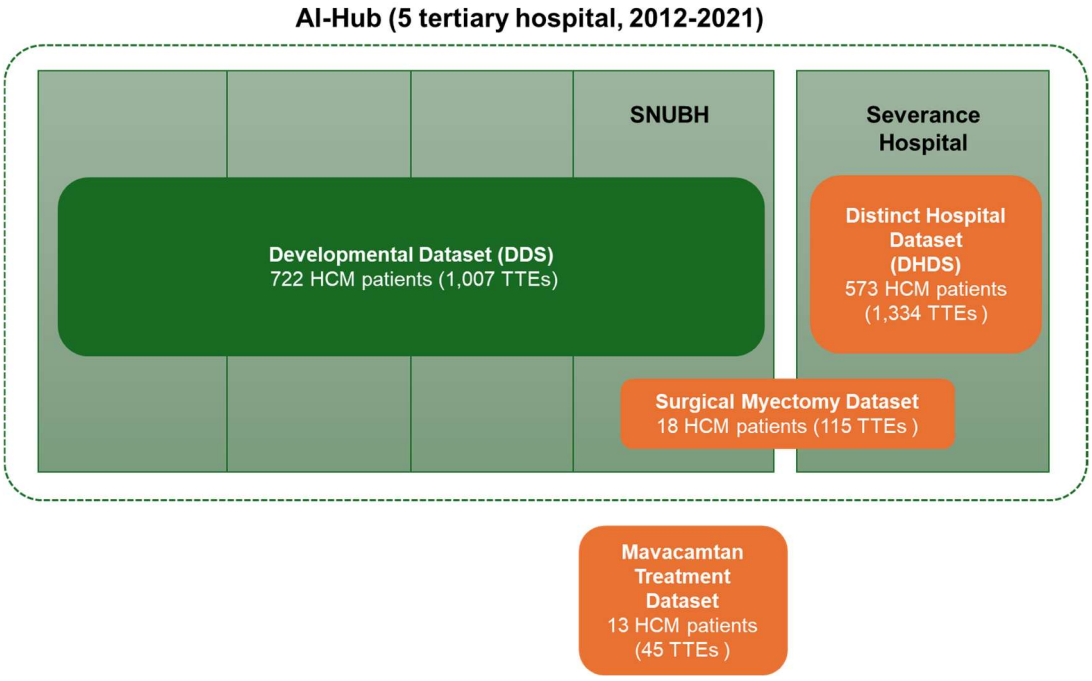

**Figure 2. DL Framework for LVOT Obstruction Assessment**

CNN, convolutional neural network; DL, deep learning; LVOT, left ventricular outflow tract; LVOTO, left ventricular outflow tract obstruction; PG, pressure gradient.

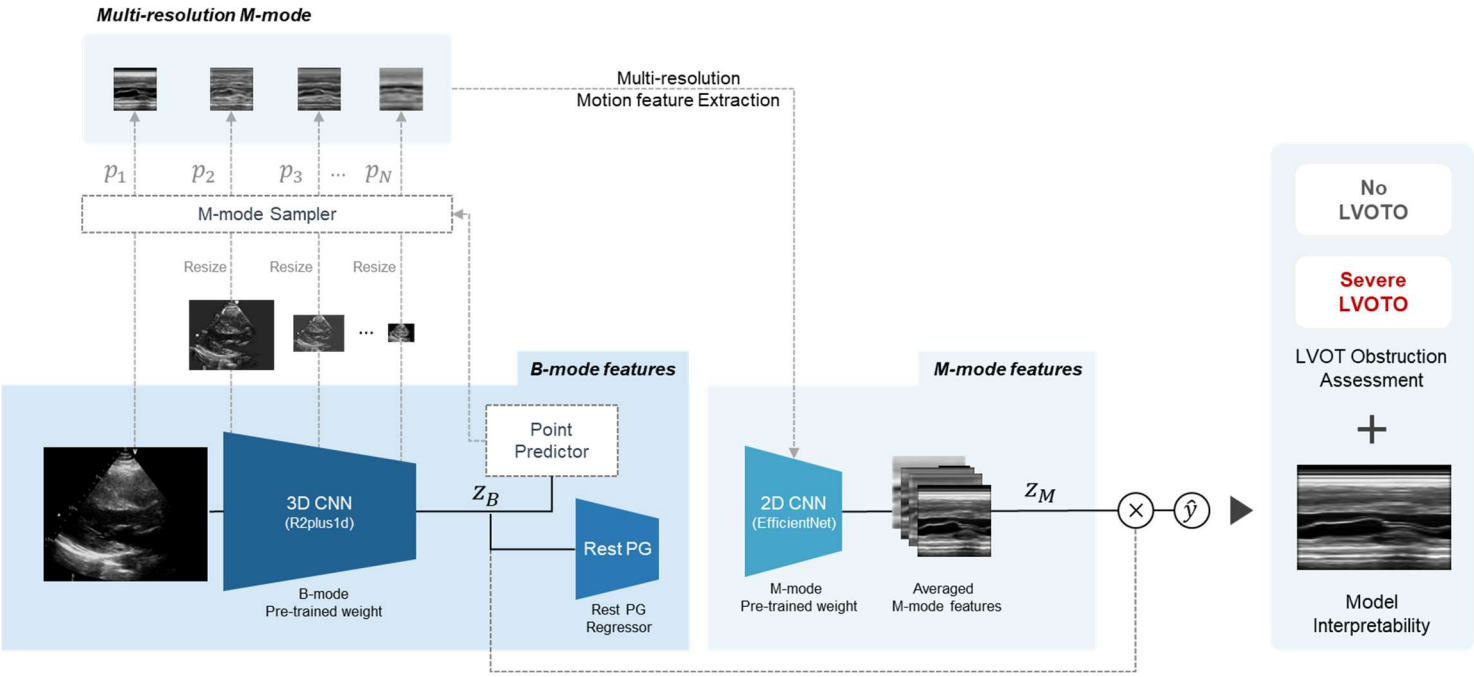

**Figure 3. Model performance in the internal and external validation sets**

DHDS, distinct hospital dataset; DLi-LVOTO, deep learning index for LVOTO; ITDS, internal test dataset; LVOTO, left ventricular outflow tract obstruction.

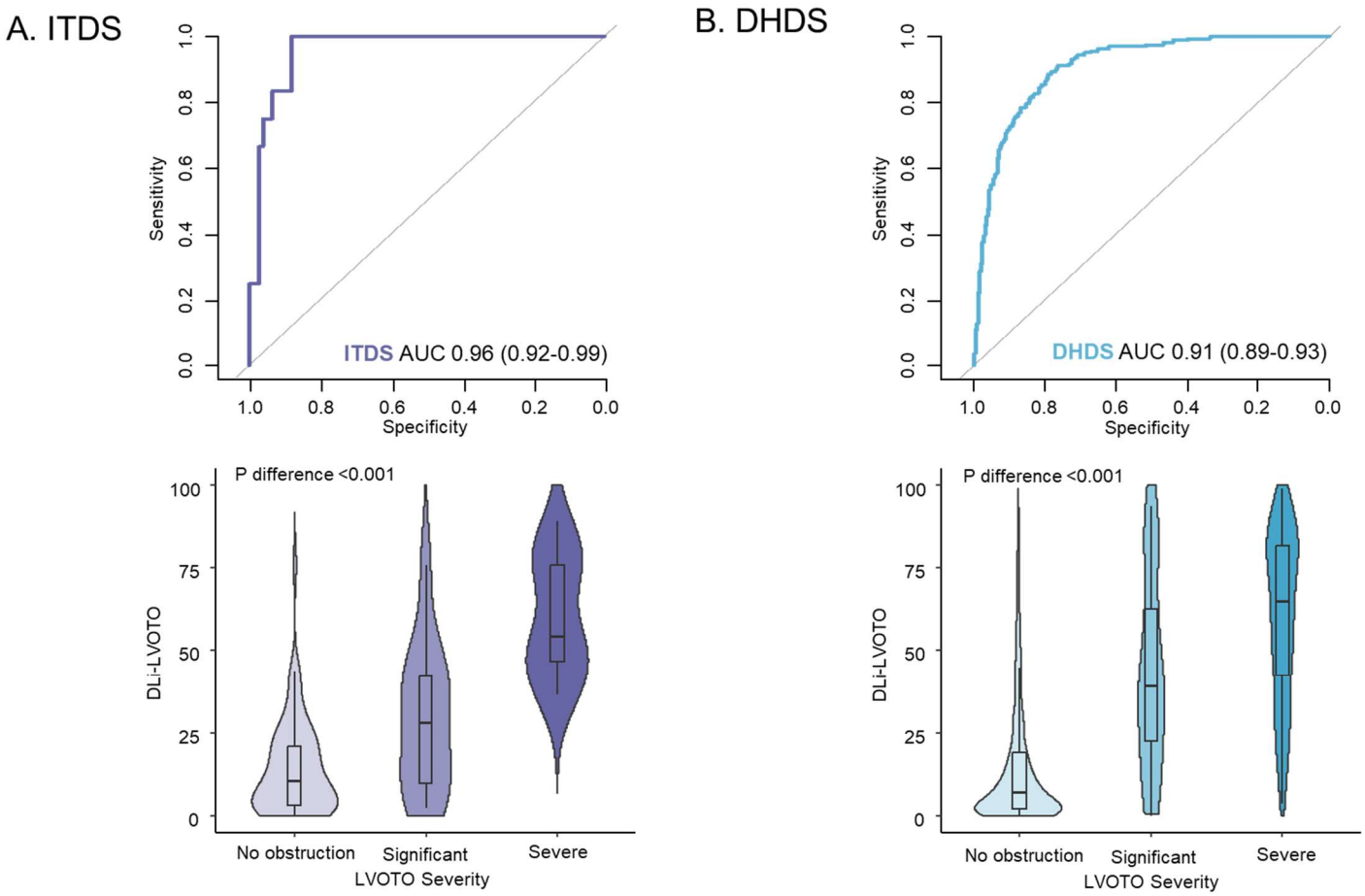

**Figure 4. Explainability Analysis for DLi-LVOTO using Saliency Map**

DHDS, distinct hospital dataset; DLi-LVOTO, deep learning index for LVOTO; ITDS, internal test dataset; LVOTO, left ventricular outflow tract obstruction.

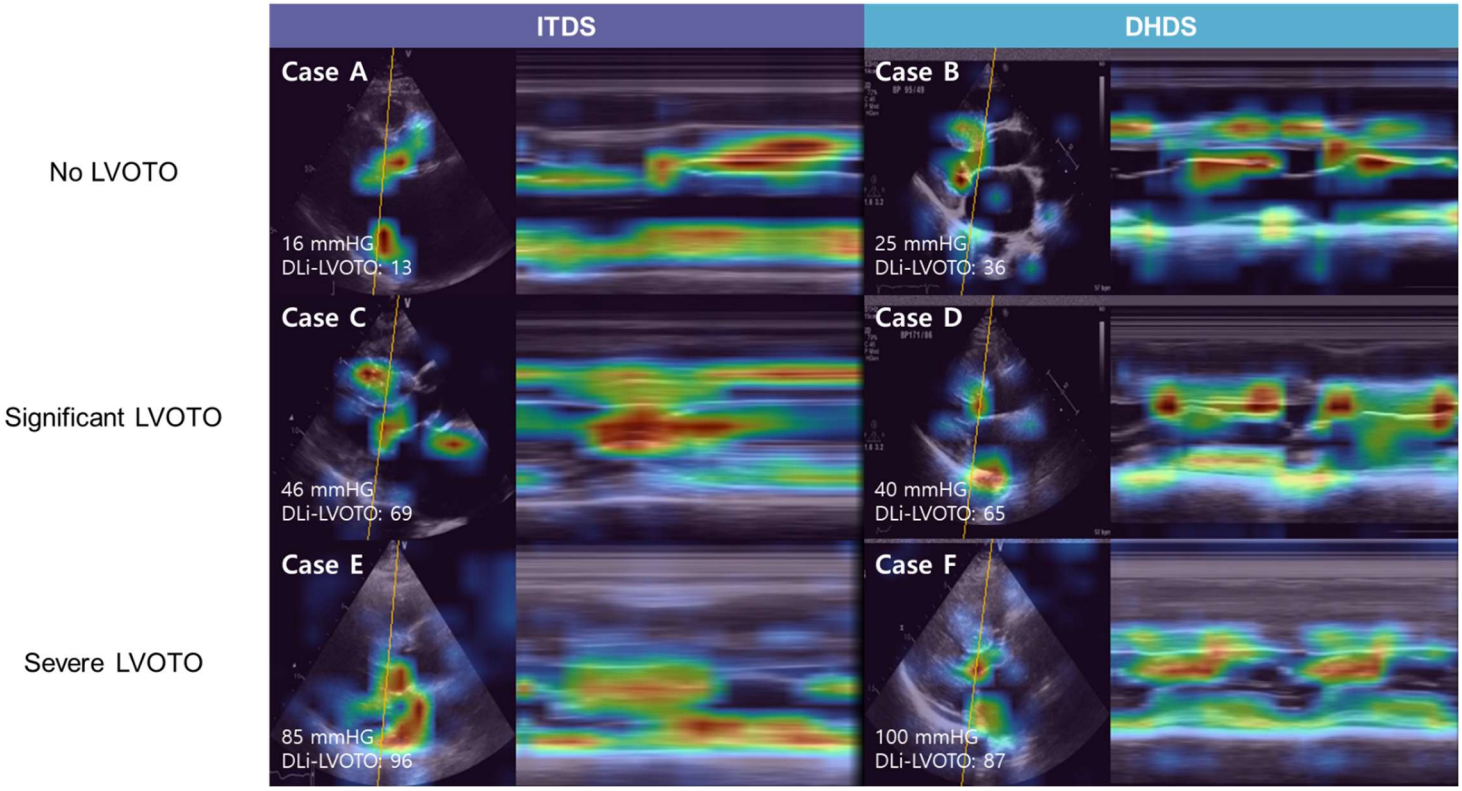

**Figure 5. Interval changes in DLi-LVOTO and peak PG after LVOT Gradient Reduction Treatment**

DLi-LVOTO, deep learning index for LVOTO; LVOT, left ventricular outflow tract; PG, pressure gradient.

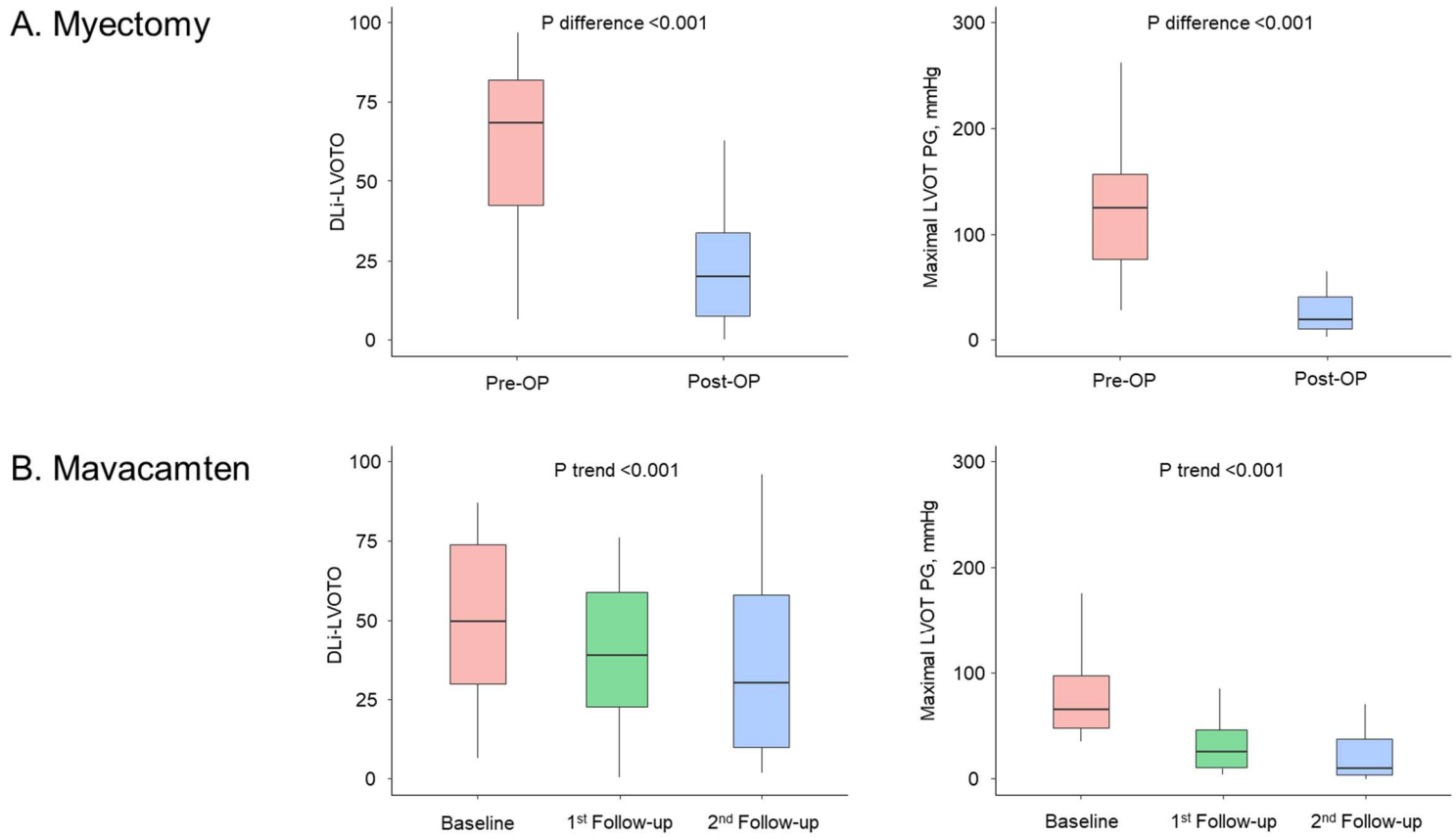

**Figure 6. Representative Cases for Trends in DLi-LVOTO and PG with LVOT Gradient Reduction Treatment**
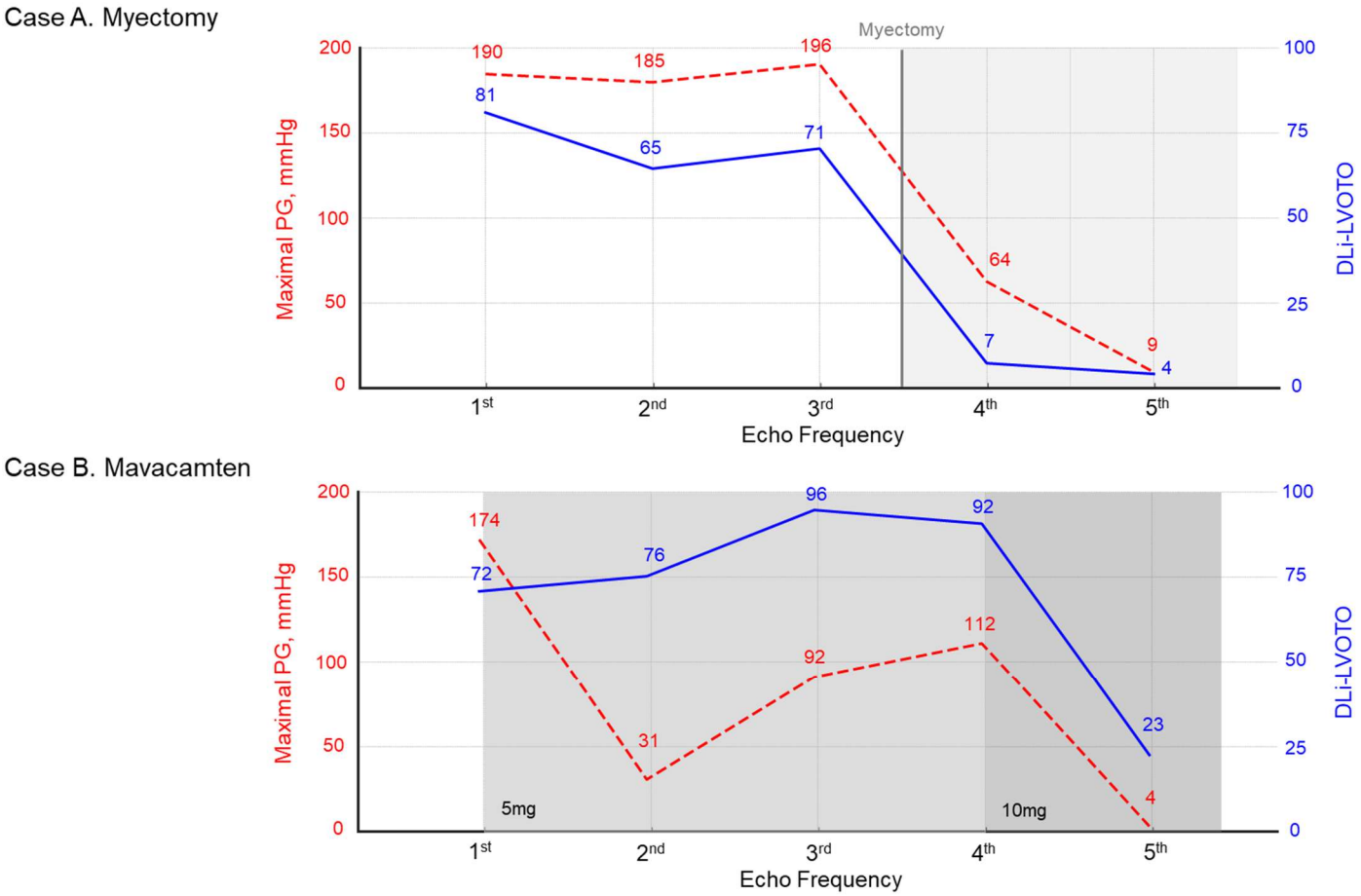
DLi-LVOTO, deep learning index for LVOTO; LVOT, left ventricular outflow tract; PG, pressure gradient.